

EPFD Measurements on GPS and Iridium at the RPA

Nia Imara

July 2002

ABSTRACT

The 3.2 m diameter reflectors of the RPA are well calibrated in absolute gain, antenna pattern and system noise temperature, and can therefore be used to characterize the EPFD of multiple satellite systems. Power flux densities of both the GPS near 1575 MHz and the paging signal of the Iridium satellite system near 1626.4 MHz were measured with one of the RPA antennas, once with the antenna pointing at zenith and once with the antenna pointed at lower elevation. In each case, the satellites were monitored for no less than 1.5 days. A boxcar average later provided a view of the power flux densities and occurrence probabilities with an integration time of 2000 s. Statistical distributions of power flux density were found for each of the satellite systems. In particular, the power flux density levels exceeded 2% of the time varied little (about 1 dB) with the antenna elevation angle. At the 2% probability level, GPS and Iridium power flux densities were observed to be -181 dB(W/m²/Hz) and -186 dB(W/m²/Hz) at 1575 MHz and 1626.4 MHz, respectively. These values should be compared with the ITU detrimental limit of -238 dB(W/m²/Hz), which these satellites should not exceed at 1612 MHz. A later study should extend the statistical sampling to other pointing directions, and compare the detailed results with those predicted by theoretical EPFD modeling studies, for which the results of this study have now provided a sample of 'ground truth'.

INTRODUCTION

Systems such as the Global Positioning System (GPS) and Iridium require multiple satellites above the user's horizon to carry out their intended purpose. The International Telecommunications Union (ITU) recognizes the need to evaluate potential interference to other services such as the Fixed Satellite Service (FSS) and the Radio Astronomy Service (RAS) from such systems. The Equivalent Power Flux Density (EPFD) method has been developed within the ITU to address this issue of multiple entry, that is, the simultaneous arrival at a receiving antenna of signals from several satellites. The EPFD algorithm¹ is

$$EPFD = 10 \cdot \log_{10} \left[\sum_{i=1}^{N_a} 10^{10} \cdot \frac{P_i}{4\pi d_i^2} \cdot \frac{G_t(\theta_i) \cdot G_r(\phi_i)}{G_{r,max}} \right]$$

¹ International Telecommunication Union, Document 7D/47, (2001)

where:

- N_a : is the number of non-geostationary space stations that are visible from the radio telescope;
- i : is the index of the non-GSO space station considered;
- P_i : is the RF power of the unwanted emission at the input of the antenna (or RF radiated power in the case of an active antenna) of the transmitting space station considered in dBW in the reference bandwidth;
- θ_i : is the off-axis angle between the boresight of the transmitting space station and the direction of the radio telescope;
- $G_t(\theta_i)$: is the transmit antenna gain (as a ratio) of the space station in the direction of the radio telescope;
- d_i : is the distance in meters between the transmitting station and the radio telescope;
- ϕ_i : is the off-axis angle between boresight of the radio telescope and the direction of the transmitting space station considered in the non-GSO system;
- $G_r(\phi_i)$: is the receive antenna gain (as a ratio) of the radio telescope, in the direction of the transmitting space station considered in the non-GSO system;
- $G_{r,max}$: is the maximum gain (as a ratio) of the radio telescope;
- $EPFD$: is the instantaneous Equivalent Power Flux Density in dB(W/m²) in the reference bandwidth at the radio telescope.

In the case of the Radio Astronomy Service, ITU Recommendation RA.769 states that, “For a given cell, if the PFD threshold level is not exceeded for more than 98% of the EPFD samples, then interference to the Radio Astronomy Service is considered acceptable.”² In order to evaluate the levels of EPFD exceeded not more than 2% of the time, EPFD modeling calculations use extensive computing resources because of the statistical character of the results. As a complement to such calculations, the present study provides ‘ground truth’ measurements using a well calibrated receiving antenna. These measurements can be used to validate the results of theoretical studies.

METHOD AND ANALYSIS

The measurements described here were made using the Rapid Prototype Array (RPA), which is a small radio interferometer near Lafayette, California. The RPA consists of seven 3.2 m dishes, and all of the measurements described here were taken with a single dish (RPA6).

The EPFD is expected to vary depending on the pointing direction of the telescope for two reasons. Firstly, it will depend on elevation angle, θ , because the distance to the satellite depends on θ and because the transmit gain of satellites intersecting the main beam varies with θ .

² ITU Recommendation RA.769, (2001)

Secondly, if the satellite orbital period is commensurate with earth's rotational period, there may be some (azimuth, elevation) settings where no satellites ever intersect the telescope main beam. In this case, the EPFD varies strongly and rapidly with pointing direction.

Over long sampling periods with Iridium, only the first pointing dependence applies because the instantaneous longitudinal separation of the 80+ satellites is comparable to the telescope's beam width (FWHM 4°). Also, the Iridium orbital period is incommensurate with earth's rotational period. By comparison, EPFD measurements of GPS are subject to both pointing dependencies since the GPS period is exactly half the rotational period and because the longitudinal separation of the 24 GPS satellites (15°) is much larger than the RPA beam width.

This means that a complete sampling of the EPFD from GPS will require hundreds of pointings and/or some theoretical extrapolation. (Notice that only 24-hour data accumulation is required for each pointing since the GPS EPFD is periodic.) To begin this process, we focus on two pointings: one at zenith and another elevation near the lower limit of the RPA drive. To determine reasonable coordinates for the latter direction, a satellite was tracked until the antenna reached a desirable position, thus ensuring that at least one satellite was in the main beam. The low point was (azimuth, elevation) = $(276^\circ, 35^\circ)$ for GPS.

A complete sampling of Iridium's EPFD could be accomplished with 10 to 20 pointings provided that each one was sampled for several days. Again, we only begin such a study using two pointings, at zenith and at $(2.3^\circ, 49.9^\circ)$. Figure 1 shows the low pointings of GPS and Iridium superimposed on a graph of terrain elevation as viewed from the antenna we used (RPA6).

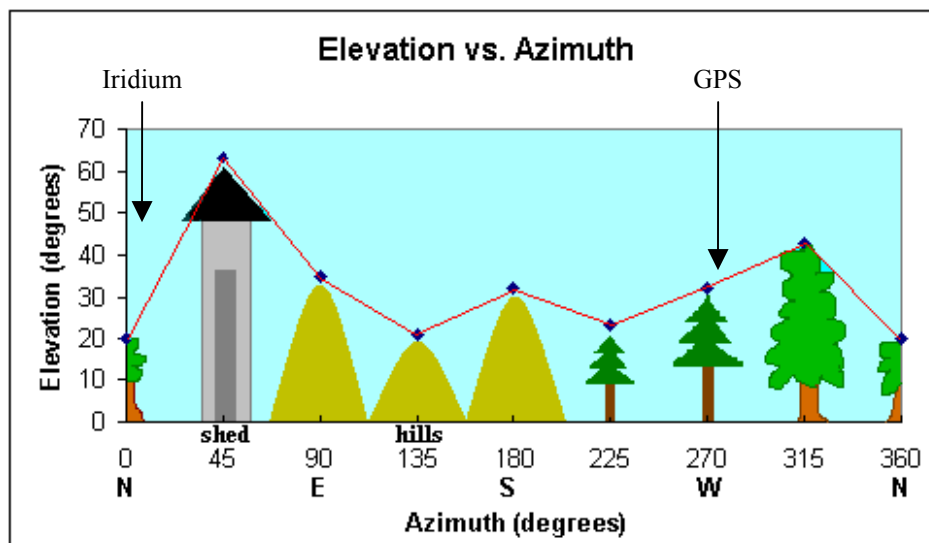


Figure 1: Plot of elevation vs. azimuth for RPA6

GPS transmits two carrier signals in the L-band. They are designated L1 (1575.42 MHz) and L2 (1227.60 MHz). We measured the power levels of the former. Iridium transmits

between 1620 and 1630 MHz, and our measurements were taken at 1626.4 MHz. Figure 2 shows the bandpass of RPA6 and the respective locations of the two satellite signals of interest.

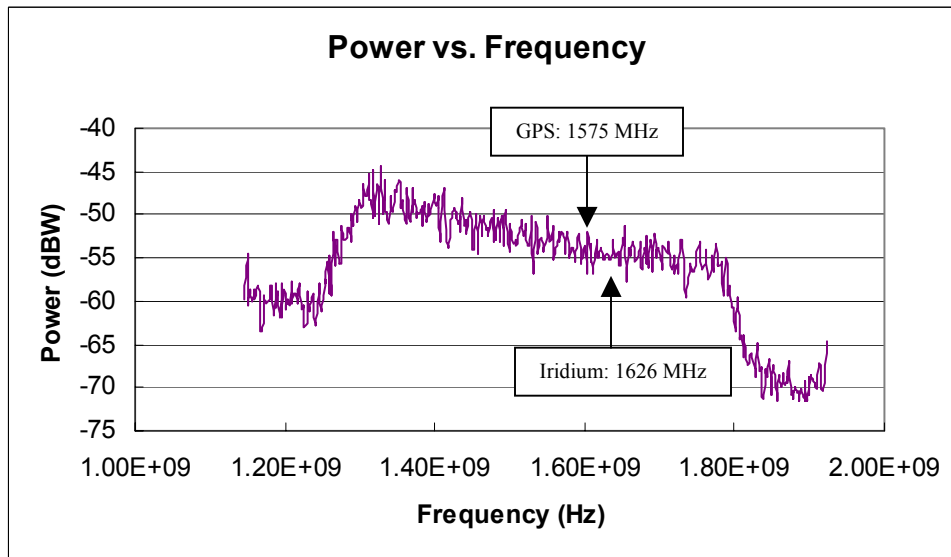


Figure 2: Plot of power vs. frequency showing the bandpass filter of approximately 1.200 to 1.800 GHz.

Figure 3 shows a plot of the antenna pattern of one of the RPA dishes. The effective area of the dish (4.9 m^2) can be determined from this graph.³ As mentioned earlier, the FWHM of the antenna gain is about 4° and the gain drops below isotropic levels at angles greater than 12° from beam center.

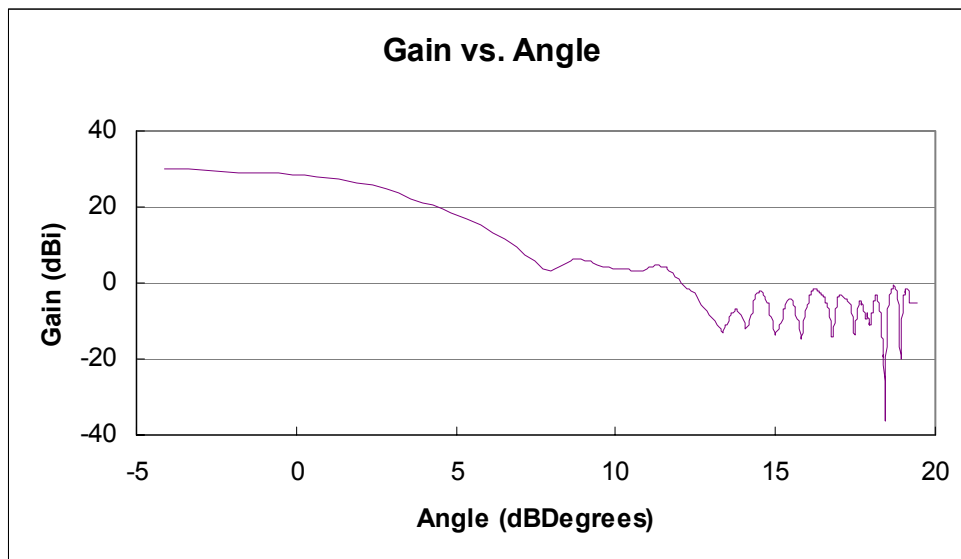


Figure 3: Plot of antenna gain vs. angle measured from boresight.

³ See G.R. Harp and R.F. Ackerman, *Mapping the Antenna Gain at the RPA*, (2001)

Figure 4 displays the setup of the electronics. After being collected by the antenna, the signal was sent through a low noise amplifier. Any frequencies outside of approximately 1200 to 1800 MHz were filtered out by the bandpass filter (Figure 2). The spectrum analyzer then did a spectral analysis on the signal. Finally, a computer program recorded a power spectrum vs. frequency every 10 s.

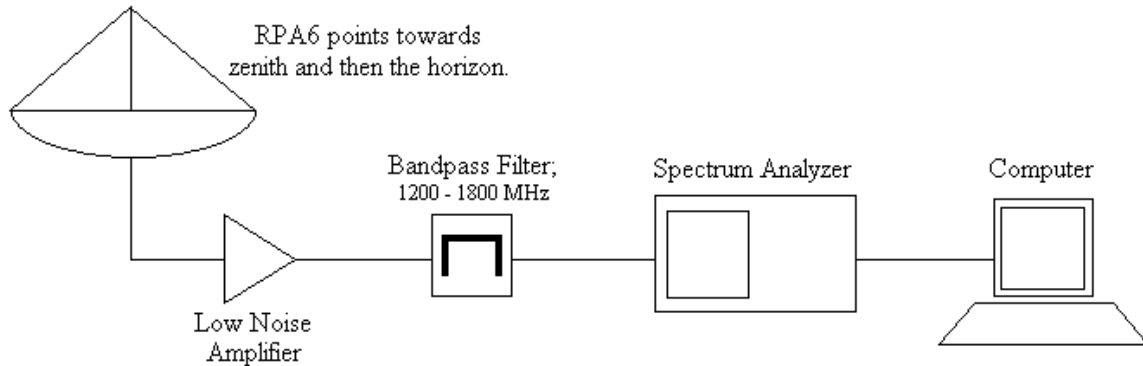


Figure 4: Block diagram of electronics.

Two different methods were employed for the analysis of the GPS and Iridium data. The GPS analysis will be discussed first.

GPS

The spectrum analyzer was tuned to a center frequency of 1575 MHz and a bandwidth of 10 MHz. Table 1 displays all of the parameters used to set up the spectrum analyzer for GPS.

Spectrum analyzer parameters for GPS	
Average powers	On
Average count	100
Starting frequency	1.570 GHz
Stopping frequency	1.580 GHz
Video bandwidth	100 kHz
Resolution bandwidth	100 kHz
Reference level	-20 dB
Sweep time	5 ms

Table 1

Since we were interested in the total power transmitted by GPS, integration was performed over the range of 1574 to 1577 MHz for each spectrum, (the spectrum analyzer processes one spectrum every 10 s). See Figure 5 and note that the range of 3 MHz was chosen to fully encompass the peak of the GPS spectrum.

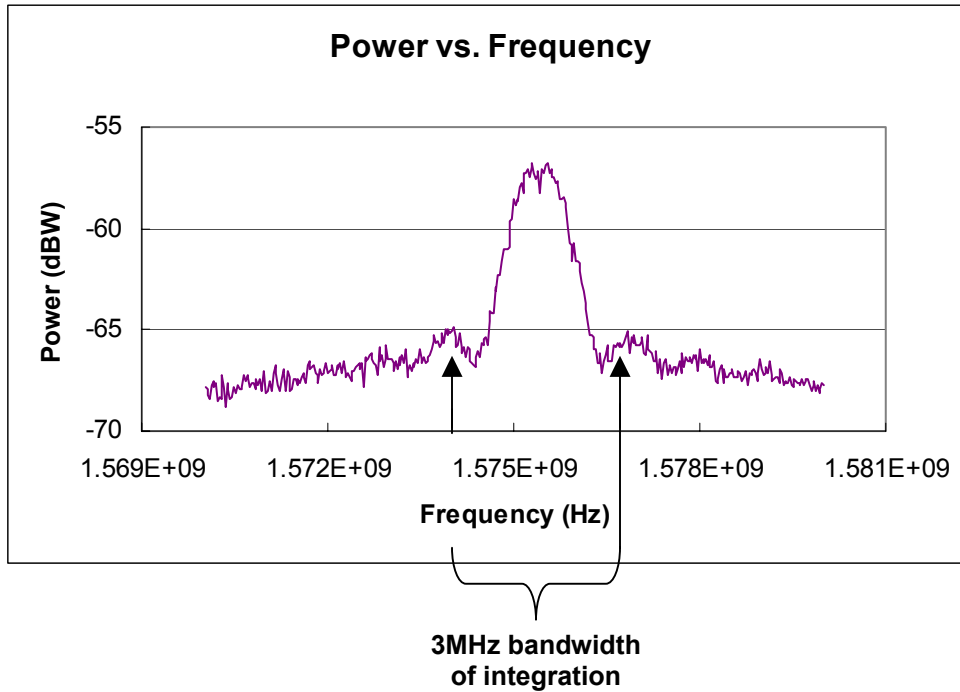


Figure 5: A plot of the GPS spectrum when a satellite is close to the center of the beam.

It is important to note that the power was converted to the linear scale before the integration was performed. After this, it was converted back to dBW.

Next, in order to find the EPFD with respect to time, the raw values of power acquired by the spectrum analyzer were divided by the effective area of the dish and then multiplied by the ratio of the system temperature (290 K) to the measured system noise floor (measured on an empty patch of sky). This, in turn, was normalized for the bandwidth of integration (3 MHz).

Once again, it is important to note that conversions had to be made between the linear and logarithmic scales before certain operations were performed. Here, all values were first converted into dB units. Figure 6 displays a sample calculation:

LINEAR
 $EPFD = \text{raw power} \cdot \text{normalized system temperature} / \text{effective area}$
 where $\text{normalized system temperature} = \text{system temperature} \cdot \text{bandwidth of integration} / \text{average noise}$

LINEAR to dB
 $x \text{ units} = 10 \cdot \log(x \text{ units})$ $\text{dB units} = y \text{ dB units}$

dB
 $PFD = \text{raw power} + \text{normalized system temperature} - \text{effective area}$
 where $\text{normalized system temperature} = \text{system temperature} + \text{bandwidth of integration} - \text{average noise}$

$P = kTB$ where P is power, k is Boltzman's constant, T is temperature, and B is bandwidth.

Thus, $P/B = kT \Rightarrow \text{system temperature is } 290 \text{ K} \cdot k = -204 \text{ dB}(W/Hz)$.

Let $\text{average noise} = -4.5 \text{ dBW}$ and $\text{raw power} = -4.3 \text{ dBW}$.

$\therefore EPFD_{\text{sample}} = -146 \text{ dB}(W/m^2)$

Figure 6: Description of the data analysis procedure.

Figures 7 and 8 display these values plotted against modified Julian day (MJD). RPA6 monitored GPS at zenith for approximately 3 days and at elevation 35° for approximately 1.5 days. In Figure 7, especially, one can observe the 24-hour periodicity of the GPS signal that was mentioned above.

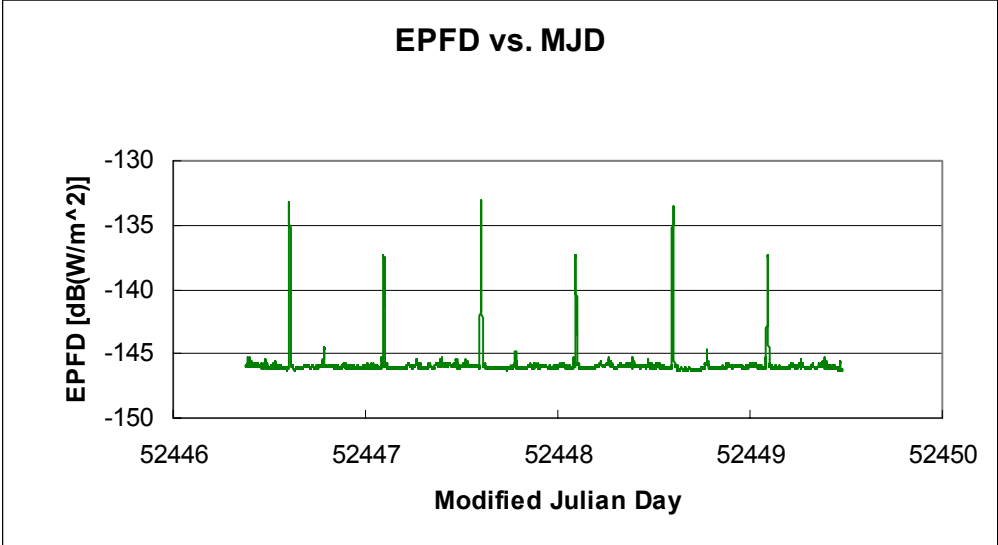


Figure 7: Plot of EPFD vs. MJD for GPS with RPA6 at elevation = 90°.

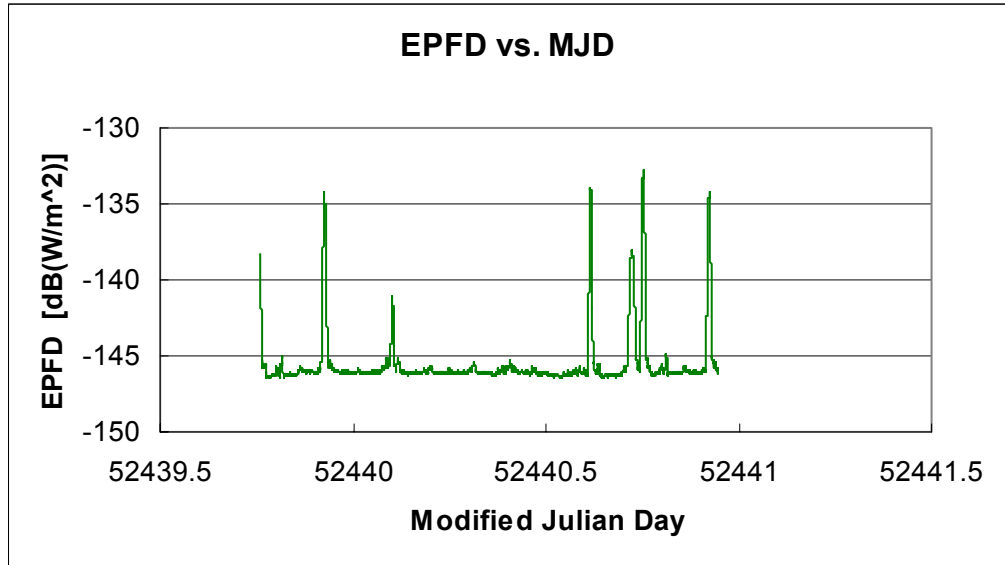


Figure 8: Plot of EPFD vs. MJD for GPS with RPA6 at azimuth = 276° and elevation = 35°.

Iridium

Table 2 lists the parameters used when monitoring Iridium. Notice that a span of zero was used here, as opposed to a bandwidth of some width as with GPS. In this case, the effective bandwidth of the measurement is about 1 kHz—the setting of both the resolution and video bandwidth.

Spectrum analyzer parameters for Iridium	
Average powers	On
Average count	25
Center frequency	1.62648 GHz
Span	0
Video bandwidth	1 kHz
Resolution bandwidth	1 kHz
Reference level	-25 dB
Sweep time	400 ms

Table 2

Because of the rapidity with which Iridium transmits its signals, we were faced with the problem of choosing between using a span of finite width or a span of zero. Had we chosen a finite span, we would have missed valuable data while the spectrum analyzer was traversing the range of frequencies—that is, Iridium might be pulsing at one frequency while we were collecting data at another point in the spectrum.⁴ Thus, we

⁴ This is not an issue for GPS measurements because GPS satellites move very slowly (0.5% min, maximum) and because the GPS power output is nearly constant.

decided to use zero frequency span and let the spectrum analyzer continuously record the total power received at one frequency. The value for the center frequency was determined by locating the frequency at which the maximum power was transmitted by an arbitrary satellite tracked beforehand near zenith. Evidently, much data was missed using this method as well, since we could not sum up the power transmitted by Iridium at any other frequency. But because one of our primary concerns here was to find the maximum power output by the satellites, this method was preferable to the former.

There were two main differences between the EPFD calculations for Iridium and GPS. First, Iridium values for *raw power* were the result of summing all of the power received in a single frequency bin over a 10 s period, instead of integrating as with GPS. (In the Iridium case, each summation was also divided by 401, the number of points swept by the spectrum analyzer.) Second, the power was normalized to the resolution bandwidth (1 kHz) instead of the nonexistent bandwidth of integration.

Figures 9 and 10 present the Iridium plots with RPA6 at zenith and at elevation 49.9°. Their durations are a little under 3 and 2 days, respectively. Notice that there is no evidence of commensurate periodicity in these spectra as was expected for Iridium.

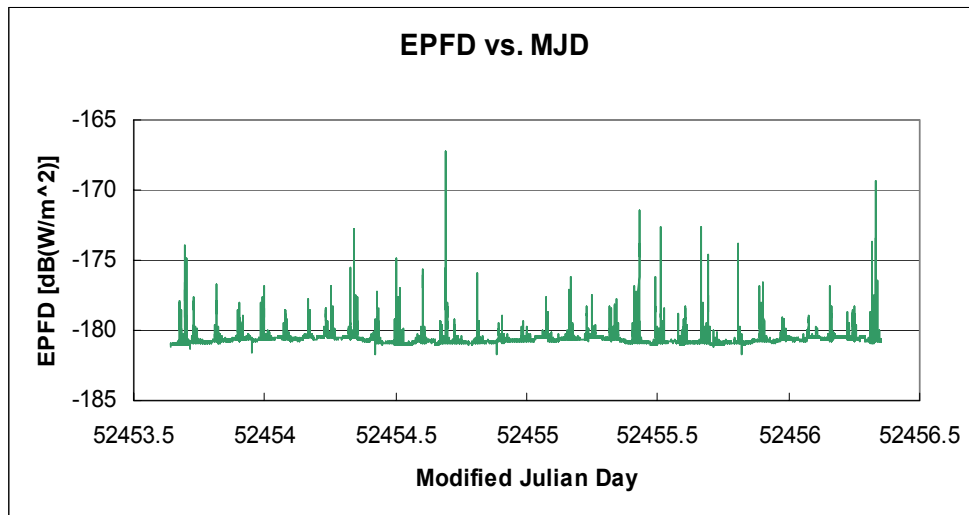


Figure 9: Plot of EPFD vs. MJD for Iridium with RPA6 at elevation = 90°.

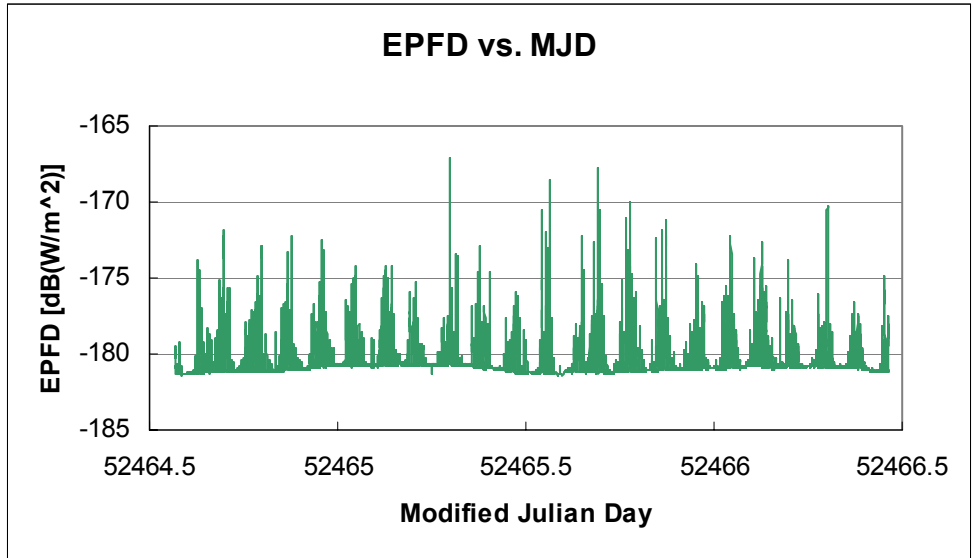


Figure 10: Plot of PFD vs. MJD for Iridium with RPA6 at azimuth = 2.3° and elevation = 49.9°.

RESULTS

The maximum power detected with RPA6 at zenith *and* at elevation 35° was -133 dB(W/m²). Because we made sure that GPS passed through the main beam for the low elevation data, we are confident that a satellite passed through the main beam for the zenith data, as well, since we get a nearly identical peak power for both sets of data.

Figure 11 shows an expanded view of a GPS peak event. This spectrum shows how stable the GPS power is and that its signal is well sampled using a 10 s time integral.

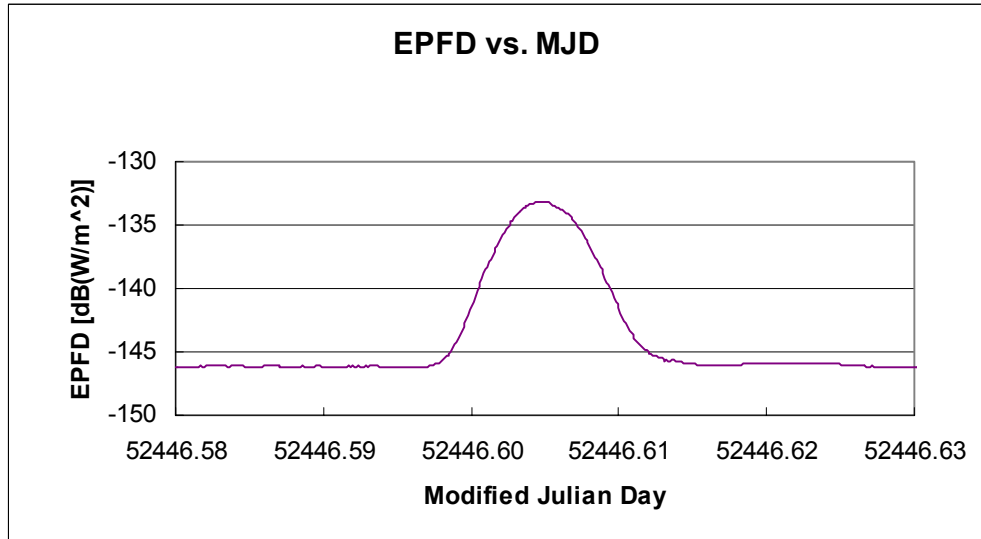


Figure 11: Plot of a GPS peak event over approximately a 1 hour period with RPA6 pointing at zenith.

For RPA6 pointing at zenith, one can see in Figure 7 that there are two significant events per day, occurring roughly 12 hours apart. At low elevations, however, the number of peak events increases by more than twofold. This is in good agreement with expectation. The projection of the telescope primary beam on the spherical shell containing the GPS satellites has twice the area at $\theta = 35^\circ$ as compared to $\theta = 90^\circ$. Figure 8 shows five major events per day, with the smallest peak occurring at about $-141 \text{ dB(W/m}^2\text{)}$. That more peak events are detected lower elevation is a truth also apparent in Figure 12, where we display the 10 s EPFD calculated as in Figure 6.

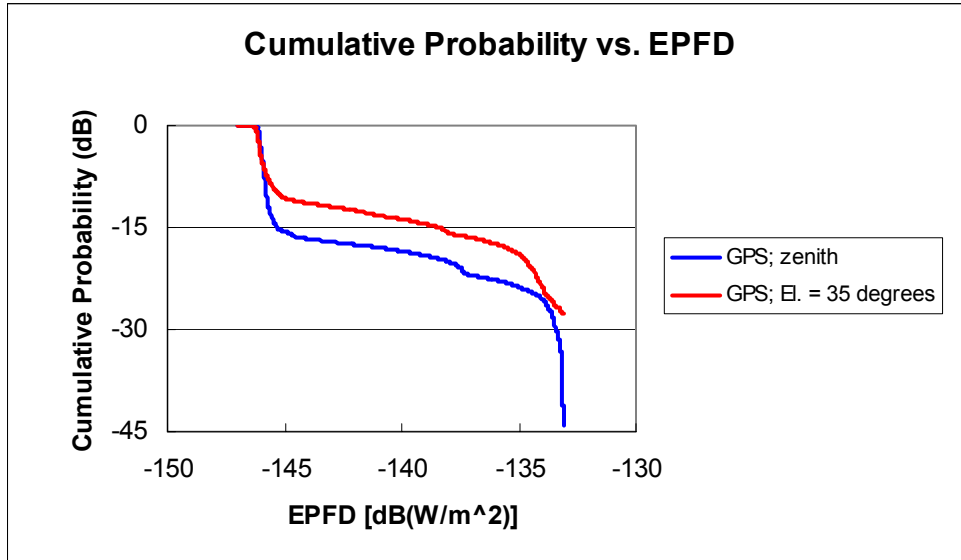


Figure 12: Occurrence probability of events for GPS.

Because Iridium satellites orbit much closer to the earth and there are more of them, (as compared to GPS), the time any one satellite spends in the antenna primary beam is only a few seconds, as depicted in Figure 13. Notice that the abscissa of Figure 13 spans the same time period as in Figure 11. Nevertheless, our zero-span measurement technique does an adequate job of capturing Iridium peak events.

As with GPS, the maximum power measured from Iridium at the two elevation angles (Figures 9 and 10) was nearly identical, $-1.67 \text{ dB(W/m}^2\text{)}$. And although Iridium's orbital period is not commensurate with earth's rotation, there is an obvious pseudo-periodicity in the data with a frequency of about 11 cycles per day. This unexpected fact gives us confidence that even with only a day or two of observations, we have adequately sampled Iridium's power spectrum for each pointing.

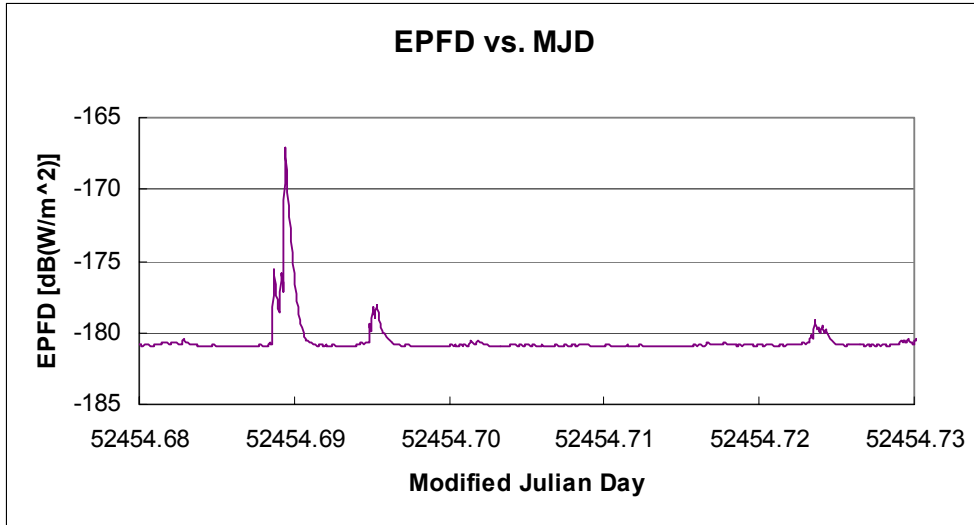


Figure 13: Plot of an Iridium peak event over approximately a 1 hour period with RPA6 pointing at zenith.

Figure 14 shows the 10 s EPFD results for iridium at the two elevations. As with GPS, the occurrence of high-power events rises markedly as the antenna is lowered toward the horizon.

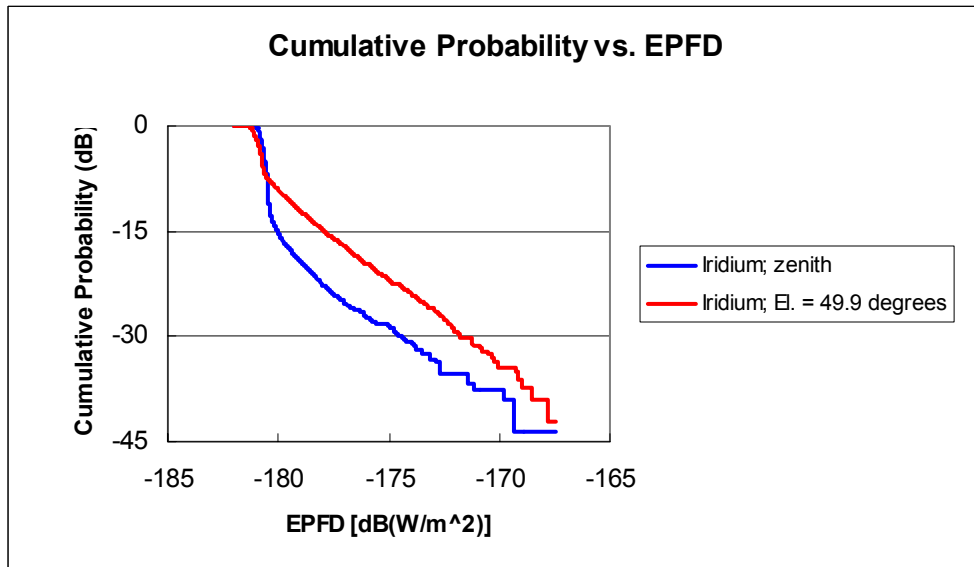


Figure 14: Occurrence probability of events for Iridium.

The more standard integration period used by radio astronomers and the ITU is 2000 s. Thus, Figures 15 through 20 display new graphs of EPFD vs. MJD and occurrence probability arrived at applying a 2000 s boxcar average to the data in Figures 7-10.

As one can see in the graphs displayed below, integrating over 2000 s broadens the peaks and decreases the peak-to-noise ratio significantly. This is just a reflection of the fact that GPS and Iridium satellites pass through the telescope primary beam in much less than 2000 s.

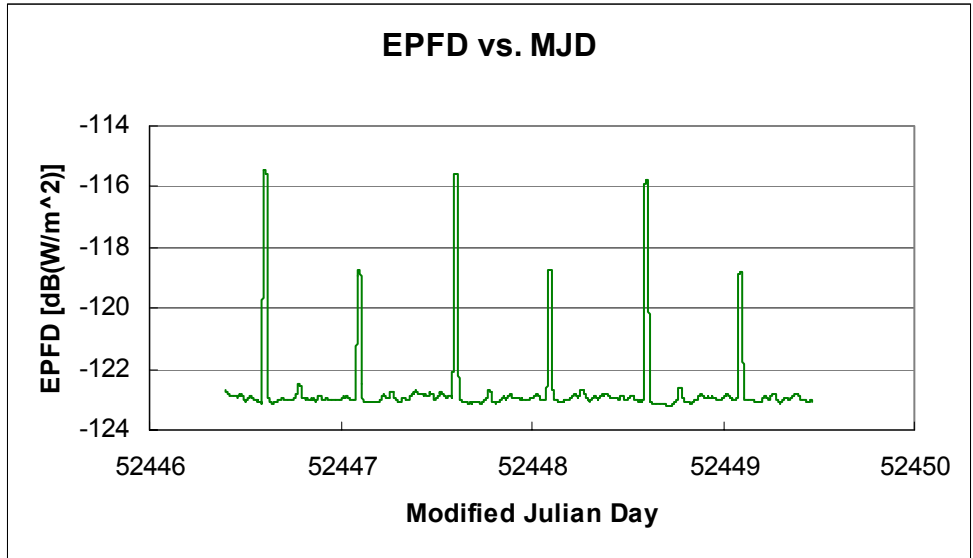


Figure 15: Plot of PFD vs. MJD for GPS with RPA6 at elevation = 35°, using 2000 s integration periods.

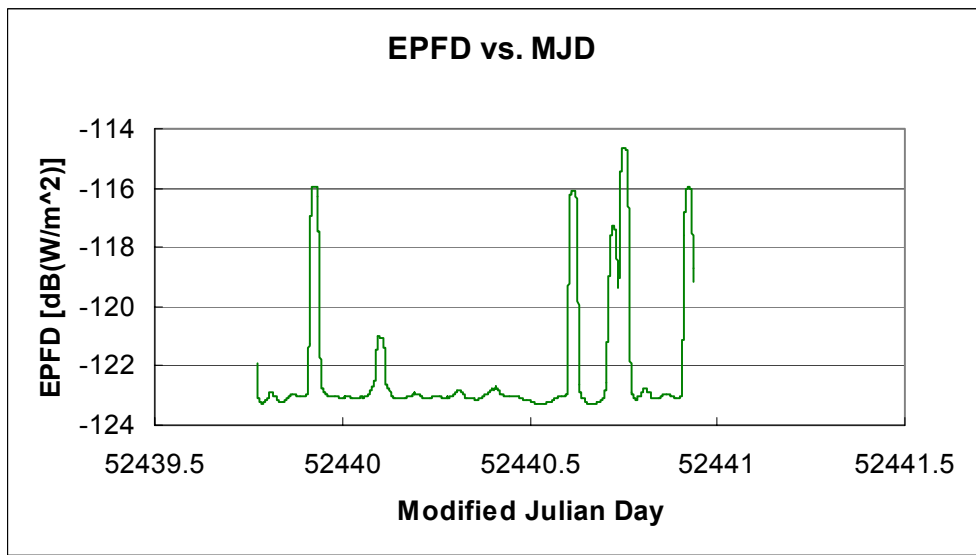


Figure 16: Plot of PFD vs. MJD for GPS with RPA6 at azimuth = 276° and elevation = 35°, using 2000 s integration periods.

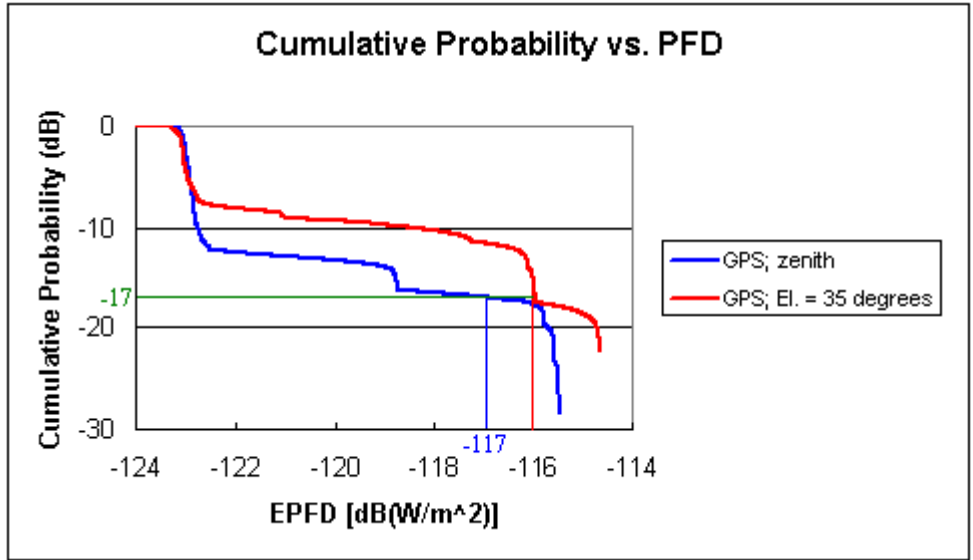


Figure 17: Occurrence probability plot for GPS based on Figures 15 and 16.

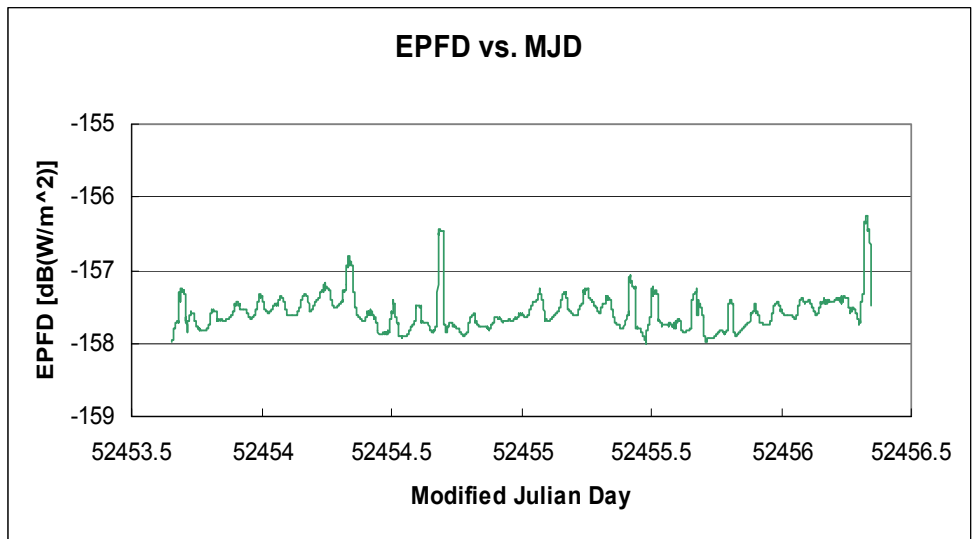


Figure 18: Plot of PFD vs. MJD for Iridium with RPA6 at elevation = 0°, using 2000 s integration periods.

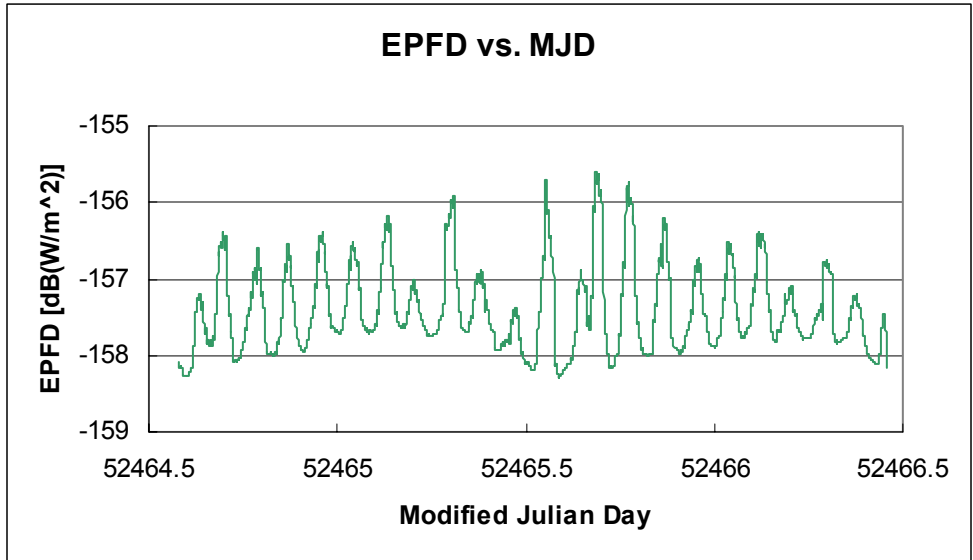


Figure 19: Plot of PFD vs. MJD for Iridium with RPA6 at azimuth = 2.3° and elevation = 49.9°, using 2000 s integration periods.

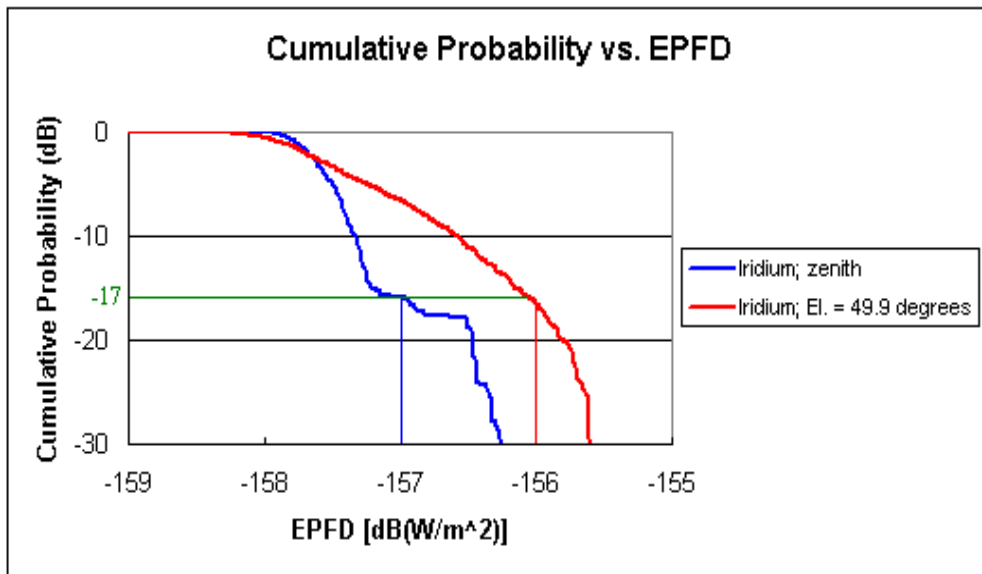


Figure 20: Occurrence probability plot for Iridium based on Figures 18 and 19.

Notice that in all the EPFD plots, the noise floor rises up and down with a 24-hour period and peaking shortly after noon. This is especially evident in Figure 19 and is due to a fluctuation in system temperature correlated with the outside air temperature. (Note that RPA amplifiers and electronics are not temperature controlled.)

DISCUSSION AND CONCLUSION

Figures 17 and 18 mark off the 2% level ($0.02 = -17$ dB) in the intended satellite transmitting band. From the difference between this level and the detrimental threshold level inside the radio astronomy band we can calculate the attenuation required between these two frequencies to prevent detrimental interference.

For example, the 2% probability level of the GPS signal, when RPA6 is pointed at elevation 35° , is -116 dB(W/m²) averaged over 3 MHz, or -181 dB(W/m²/Hz). Now, the nearest protected radio astronomy band to GPS and Iridium signals is at 1612 MHz. The ITU states that the detrimental level there is -238 dB(W/m²/Hz).⁵ Hence, the GPS satellite system will not cause detrimental interference more than 2% of the time if its signal level is attenuated by at least 57 dB at 1612 MHz or more relative to its value inside its allocated band.

Similarly, in the 1 kHz measurement band, the Iridium paging signal at the 2% probability level is -156 dB(W/m²), or -186 dB(W/m²/Hz), when RPA6 is pointed at elevation 49.9° . So the required attenuation in this case is 52 dB. However, the Iridium transmission frequency is much closer to the protected band than that of GPS. Therefore, the requirements on the Iridium signal falloff are much more stringent.

Note that for both satellite systems, the difference in PFD between zenith and a lower elevation at the 2% probability level was approximately 1 dB. Because the satellites are more distant at lower elevation, we conclude that the transmission gain, G_t , must be shaped in such a way to compensate for the $1/r$ decrease in amplitude, which we otherwise would expect. It would be interesting to see whether further studies confirm this value when the telescope is pointed in other directions.

ACKNOWLEDGEMENTS

I want to thank Gerry Harp for all of his patience, time, and support over the summer during which this paper was written and Mike Davis for all of his enthusiasm and encouragement. I also want to thank Jill Tarter for her kindness and support, as well as her generosity in providing me with this opportunity. Finally, I thank those who helped open up the very first doors leading to all of the wonderful opportunities and experiences I had this summer—Dan Wertheimer and Edna Devore.

I was amazed by your openness and kindness even before I began my first day of work at the SETI Institute and continue to be so. Thank you!

⁵ ITU, *Handbook on Radio Astronomy*, Chapter 4. Table 5, (1995)